Computational Studies of the Ground and Excited State Potentials of DMSO and H₂SO: Relevance to Photostereomutation

Jerry W. Cubbage and William S. Jenks*

Department of Chemistry, Iowa State University, Ames, Iowa 50011-3111

Received: June 20, 2001; In Final Form: September 7, 2001

A computational study on ground and excited states of dimethyl sulfoxide (DMSO) and the hypothetical molecule H_2SO is reported. Full valence CASSCF/6-311+G(3df,2p) with a multireference perturbation theory correction was used for the latter, while DMSO was examined with an active space that neglected only the CH bonds and an analogous basis set that neglected polarization functions on H. A realistic value of 41.5 kcal/mol was obtained for the ground state pyramidal inversion of sulfur for DMSO, though no directly comparable experimental value is available. Calculations were also carried out on singlet and triplet excited state surfaces of both A′ and A″ symmetry. Relaxed excited state geometries fairly near the ground state geometry were found, but perhaps more importantly, excited state stationary points were also found in C_{2v} symmetry. These were the lowest energy of any geometry on their respective surfaces. This leads to the speculation that photochemical stereomutation of alkyl sulfoxides may occur without C–S bond cleavage in a mechanism formally analogous to the photochemical cis–trans isomerization of olefins.

Introduction

Despite the commonly used representation of the SO bond in sulfoxides and other sulfinyl derivatives as S=O, sulfoxides are in many ways best described as ylides with highly polarized S–O σ–bonds whose length is shorter than an idealized S–O single bond because of electrostatics.[1] Consistent with this description, sulfur bears a a lone pair of electrons and the geometry is that of a distorted pyramidal center, with CSC and CSO bond angles tighter than the idealized 109.5°. Thus, a sulfoxide with different carbon substituents is a stereogenic center. The ease of preparation[2–4] and stability[5] of optically active sulfoxides has made them very attractive as chiral auxiliaries for organic synthesis.[6–11]

The fact that the pyramidal structure of sulfoxides retains its configurational integrity has generated considerable curiosity in understanding the conditions under which epimerization can occur. The racemization of sulfoxides with a single stereogenic center was first reported in the 19th century by Krafft and Lyons[12] and first well reviewed in 1967 by Mislow.[13] For thermal unimolecular racemization of simple systems, it is generally understood that the mechanism is by simple pyramidal inversion. The activation enthalpies for methyl *p*-tolyl sulfoxide and 1-adamantyl *p*-tolyl sulfoxide were reported to be 37 and 42 kcal/mol, respectively.[5] Inversion barriers are not known for most simple dialkyl sulfoxides because thermal elimination of virtually any sulfoxide with a *β*-hydrogen to give a sulfenic acid and an olefin occurs with a barrier of less that 35 kcal/mol.[14–17]
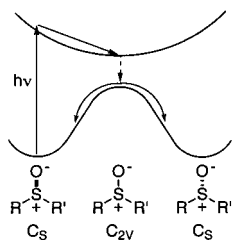
The pyramidal inversion barriers for DMSO, F₂SO, and H₂SO have been calculated by determining the difference in energy between the relaxed geometries in C_s symmetry and C_{2v} transition states.[18] For DMSO, the barrier was found to be 48 kcal/mol at the MP2/6-31+G(2d) level of theory; for F₂SO it was 39 kcal/mol. For H₂SO, it was calculated to be 40 kcal/mol at MP2/6-311G+G(2d,p). Higher levels of perturbation theory produced only minor changes.

To the best of our knowledge an "edge inversion" mechanism, which has been invoked for stereomutation of some phosphorus compounds,[19] is not known for sulfoxides. However, special structural features lead to different mechanisms of thermal stereomutation. For allyl sulfoxides, a mechanism is provided by the low-barrier reversible rearrangement to the achiral sulfenic ester.[20] With benzyl sulfoxides, racemization appears to take place through homolysis of the C–S bond.[21]

Stereomutation of sulfoxides can also be induced photochemically.[22] Restricting the discussion to directly irradiated cases, two limiting mechanisms have generally been advanced. The first derives from the well-known α-cleavage photochemistry of sulfoxides that produces an alkyl radical and a sulfinyl radical.[23–28] Reclosure of the carbon–sulfur bond from the achiral radical pair would cause net stereomutation but is accompanied by other competing reactions. However, several authors through the years have suspected that there is an additional photochemical pathway that does not involve formation of radicals.[26,29–31] The underlying idea is that geometrical relaxation in an excited state is followed by nonradiative return to the ground state, as illustrated in Scheme 1. The most convincing evidence along these lines involves molecules with demonstrably low α-cleavage product yields that nonetheless have high quantum yields for racemization,[26,30,31] but this evidence remains circumstantial. For instance, is known that methyl 1-pyrenyl sulfoxide, which photoracemizes with a reasonable quantum efficiency and suffers α-cleavage chemistry with very low efficiency, is considerably less fluorescent than either the parent arene or the corresponding sulfide and sulfone.[32] In a frozen matrix, the fluorescence quantum yield rises to 0.11, from 0.008 at room temperature. This is consistent with a nonradiative

* Corresponding author. E-mail: wsjenks@iastate.edu.

Ground and Excited State Potentials of DMSO and H$_2$SO

J. Phys. Chem. A, Vol. 105, No. 46, 2001 **10589**

SCHEME 1: Simplified Diagram for Photoracemization without Radical Formation

deactivation pathway that involves geometric relaxation. At ambient temperature, the relaxation can lead to racemization, but in the frozen glass, the motion is frozen out and fluorescence is returned to higher efficiency.

In this paper, we present a computational chemical study to test the plausibility of a mechanism like that shown in Scheme 1, using H$_2$SO and (CH$_3$)$_2$SO (DMSO) as models. To the best of our knowledge, H$_2$SO remains unobserved experimentally. However, its modest size facilitates exploration of potential surfaces. DMSO obviously does not suffer racemization experimentally, but its higher symmetry makes the computations easier than those for asymmetric sulfoxides. Though the vast majority of experimental work on sulfoxide photochemistry from our own laboratory concerns aryl sulfoxides, stereomutation of alkyl sulfoxides is also known.[33−36] We report several stationary points on the excited state surfaces and show that, indeed, structures of C_{2v} symmetry are lower in energy than those of C_s symmetry. We present evidence that the enthalpic barrier to get from the vertical (i.e., ground state) geometry to a C_{2v} geometry in certain excited states is low or zero.

Computational Methods

All computations were carried out with the GAMESS suite of programs.[37] All molecules and orbitals were viewed with MacMolPlt graphical interface for GAMESS.[38] All least linear motion paths (LLMP) were constructed using internal coordinates (Z-matrices) using MacMolPlt.

ROHF methods were used with the Boys localization protocol[39] to gain good starting orbitals for the active space of the multiconfiguration self-consistent field (MCSCF) calculations.[40] The FORS or CASSCF method was employed to find states of various configurations.[41,42] Electron correlation outside the active orbital set was recovered by using multiconfiguration quasidegenerate perturbation theory (MCQDPT).[43,44] MCQDPT allowed achievement of realistic excitation energies, since it is known that MCSCF does not compute excited state energetics accurately.[40] For simplicity, the notation MCQDPT/basis is meant to imply the single point energy at the given basis for the geometry obtained by CASSCF optimization at the same basis.

For the MCSCF and MCQDPT calculations, a full valence active space was chosen for H$_2$SO, which is 14 electrons in 10 orbitals [14,10]. For DMSO, the analogous active space leaves out only the C−H bonds, since they do not participate in the inversion. The basis sets chosen for H$_2$SO and DMSO were 6-311+G(3df,2p) and 6-311+G(3df), respectively. The difference in inversion barrier for DMSO between MCQDPT calculations done with 6-311+G(3df,2p) and 6-311+G(3df) at a fixed geometry was <0.2 kcal/mol. The same tiny difference was found for fully optimized geometries at the MP2 level of theory, as discussed below. Because of the insignificance of the p-polarization functions to the energetics and geometries, all

SCHEME 2:   H$_2$SO and DMSO Optimized Ground State Structures[a]
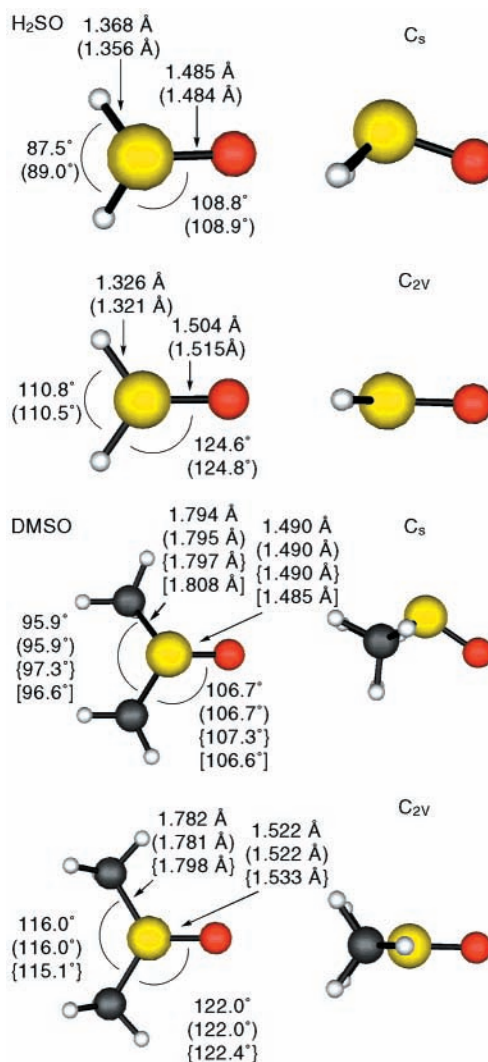
[a] For H$_2$SO, bond lengths are depicted as calculated at MP2/6-311+G(3df,2p) and (CASSCF[14,10]/6-311+G(3df,2p)). For DMSO, the bond lengths are depicted as calculated at MP2/6-311+G(3df), (MP2/6-311+G(3df,2p)), {CASSCF[14,10]/6-311+G(3df,2p)}, and [gas phase experiment].[47]

further calculations were done with the smaller basis set, which approximately halved the computation time.

The convergence of the excited singlet CASSCF wave functions was achieved by first computing the triplet CASSCF wave function using ROHF orbitals as starting orbitals, and using the triplet CASSCF orbitals as starting orbitals for the excited singlet states. It was found that the ^{1}A′ states wave function converged only with the second-order SCF (SOSCF) method.[45] The full Newton−Raphson orbital improvement (FULLNR) method was used to obtain the singlet A″ states, both triplet A′ and A″ states, and all C_{2v} excited states.[46]

Results

Ground States. *Geometries.* For both H$_2$SO and DMSO, the ground state thermal inversion is assumed to proceed from the pyramidal form with C_s symmetry (equilibrium structure) through a planar transition state (C_{2v} symmetry). These structures are shown for H$_2$SO and DMSO in Scheme 2. Bond lengths and angles calculated at different levels of theory are illustrated. Consistent with previous calculations on H$_2$SO,[18] the S−O bond

10590 *J. Phys. Chem. A, Vol. 105, No. 46, 2001*

Cubbage and Jenks

TABLE 1: Computed Ground State Inversion Barriers

method	H$_2$SO[a] (kcal/mol)	DMSO[a] (kcal/mol)
MP2/6-311+G(3df,2p)	39.1	51.0
CASSCF/6-311+G(3df,2p)[b]	58.3	
MCQDPT/6-311+G(3df,2p)[b,c]	31.9	
MP2/6-311+G(3df)		50.9
CASSCF/6-311+G(3df)[b]		67.6
MCQDPT/6-311+G(3df)[b,d]		41.5
Methyl tolyl sulfoxide[e]		37.4

[a] All values are corrected with ZPE from MP2/6-311+G(3df,2p) Hessians. [b] The active space is [14,10]. [c] Single point energy on the CASSCF/6-311+G(3df,2p) optimized geometry. [d] Single point energy on the CASSCF/6-311+G(3df) optimized geometry. [e] Experimental value in xylene.[5]

is lengthened in the planar transition state. All C_s and C_{2v} structures had zero and one imaginary frequency, respectively.

Optimized geometries for DMSO obtained using MP2/6-311+G(3df), MP2/6-311+G(3df,2p), and CASSCF[14,10]/6-311+G(3df,2p) are shown. All three levels of theory produce similar structures and are all in reasonable agreement with the equilibrium gas-phase geometry obtained from microwave spectroscopy.[47] As is reasonably expected, the CS bond lengths, SO bond lengths, and CSC bond angles and CSO bond angles are essentially unaffected by whether p-polarization functions are used on the hydrogen atoms.

Ground State Inversion Barriers. The calculated barriers to inversion for H$_2$SO and DMSO are shown in Table 1. All data include unscaled ZPEs from MP2/6-311+G(3df,2p) Hessians. For H$_2$SO, the MP2/6-311+G(3df,2p) inversion barrier is 39 kcal/mol, in good agreement with the MP2/6-311+G(2d,p) calculated values found by Fueno and colleagues.[18] The difference between the calculated barriers at Hartree−Fock (data not shown) and MP2 is comaparable to that between MCQDPT and CASSCF. The best calculated value for H$_2$SO of 31.9 kcal/mol cannot be compared to experiment.

For DMSO, the effect of the p-polarization functions on the hydrogen set was evaluated with respect to the inversion energies. As seen in Table 1, at the MP2 level of theory, the difference is negligible, and all further calculations on DMSO were done with the 6-311+G(3df) basis set. The MCQDPT/6-311+G(3df) value of 41.5 kcal/mol is at least consistent with experimental data for aryl alkyl sulfoxides.[5] To the best of our knowledge, data do not exist for the inversion barrier for simple dialkyl sulfoxides, mainly because the elimination reaction to form an olefin and a sulfenic acid occurs with a lower activation barrier when there is a β-hydrogen.

Excited States. *H$_2$SO.* In following the hypothesis represented in Scheme 1, we felt that if the vertical excited states (i.e., excited states at the ground state geometry) of the C_s structure were comparable to or higher in energy than corresponding states in planar C_{2v} symmetry, we would have a starting point, despite the limited physical meaning of the excited state at the C_{2v} ground state geometry. Singlet and triplet excited states of A′ and A″ symmetry were found at the C_s ground state geometry. The natural orbital occupation numbers (NOONs) for the active spaces of the two singlet states were 1.999, 1.999. 1.998, 1.977, 1.975, 1.990, 1.101, 0.912, 0.028, and 0.022 for the ^{1}A′ excited state and 1.998, 1.997, 1.975, 1.995, 1.998, 1.962, 1.008, 1.005, 0.043, and 0.020 for the ^{1}A″ excited state. These were fairly representative for all the excited state calculations, in that the NOONs suggested there were five nominally doubly occupied and two nominally singly occupied orbitals among the valence orbitals. Unfortunately, the singly occupied orbitals
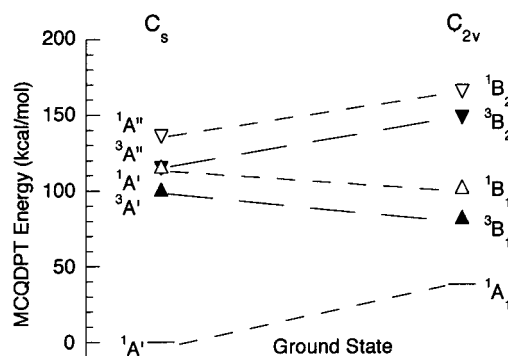
Figure 1. Excitation energies for H$_2$SO at the ground state geometries.

did not lend themselves to simple orbital descriptions of the excited states (e.g., nπ*). Applying the MCQDPT correction considerably lowered the energies of the excited states, relative to the ground state. This was a consistent phenomenon, and we will henceforth only graph or quote relative energies at that level of theory.
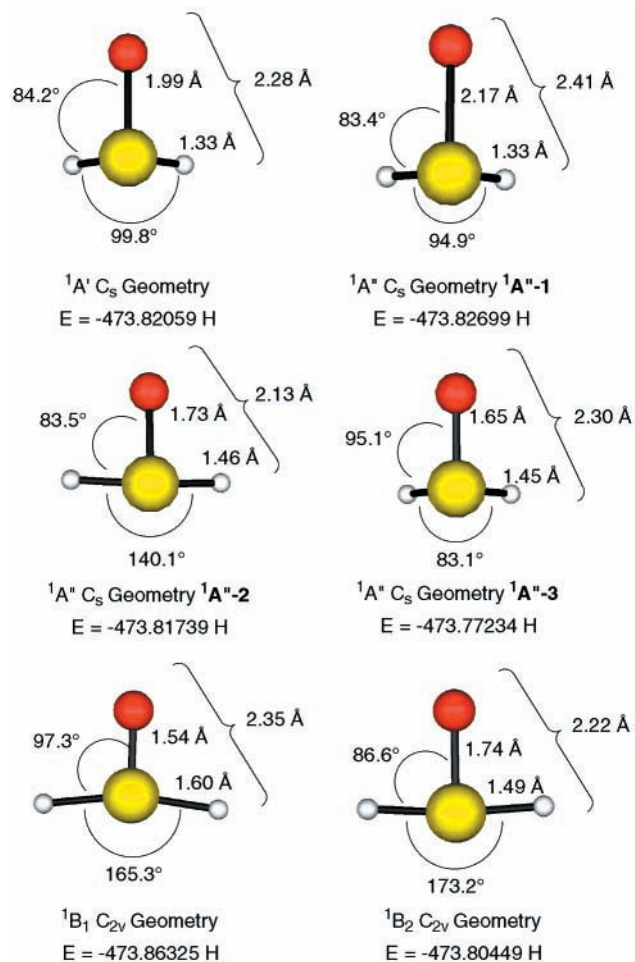
Excited states were similarly found at the C_{2v} ground state geometry. Because of the possible ambiguity about the symmetry labels in C_{2v}, we point out that by our convention, B$_1$ states in C_{2v} symmetry correspond to A′ in C_s symmetry and B$_2$ symmetry corresponds to A″ symmetry. The relative energies of these states are shown in Figure 1.

The data in Figure 1 encouraged us to continue and attempt to find optimized geometries for the excited states. Relaxed excited state geometries (i.e., stationary points in each electronic state) for the four singlet excited states (^{1}A′, ^{1}A″, ^{1}B$_1$, ^{1}B$_2$) and the four triplet states (^{3}A′, ^{3}A″, ^{3}B$_1$, ^{3}B$_2$) were obtained. Hessians were attempted to classify these states as minima, transition states, etc., but all attempts at collecting the Hessians failed. This is not atypical for excited states because while calculating the Hessian, it is necessary to remove the symmetry constraints. Thus all excited states of the same multiplicity and the ground state become the same symmetry. Convergence on the appropriate state becomes extremely difficult and calculations of vibrational frequencies usually fail. We are thus limited to the *assumption* that these geometries represent minima and cannot prove the point.

The singlet geometries and energies calculated at MCQDPT/6-311+G(3df,2p) are shown in Scheme 3. Three different stationary points with A″ state symmetry were found, which we label **^{1}A″-1**, **^{1}A″-2**, and **^{1}A″-3**, in order of ascending energy. As discussed below, these are distinct electronic states. The lowest energy excited A′ and A″ states have comparatively similar geometries, each with extended S−O bonds, S−H bonds of a length similar to the ground state, and somewhat tighter H−S−O angles.

The A″ geometries **^{1}A″-2** and **^{1}A″-3** are quite different. Structure **^{1}A″-2** is less pyramidalized and has slightly acute OSH bond angles, as does the ^{1}B$_2$ state, though the latter is necessarily planar. These latter T-shaped geometries are reminiscent of either an edge inversion geometry or a trigonal-bipyramidal structure with two of the equatorial positions occupied by nonbonding orbitals, analogous to the structures of SF$_4$ and ClF$_3$. We cannot comment further on which interpretation is more sensible at this time.

Optimization of the triplet structures only produced three bound states. Attempts to optimize an ^{3}A′ state in C_s symmetry always resulted in dissociation to H$_2$S and O(^{3}P). The optimized geometry of the ^{3}A″ state is qualitatively quite similar to the **^{1}A″-3** geometry shown in Scheme 3. The triplet structures in

Ground and Excited State Potentials of DMSO and H₂SO

J. Phys. Chem. A, Vol. 105, No. 46, 2001 **10591**

SCHEME 3: Relaxed Geometries for H₂SO Excited States[a]

[a] The energy of the C_s equilibrium structure is −473.9610427 H.

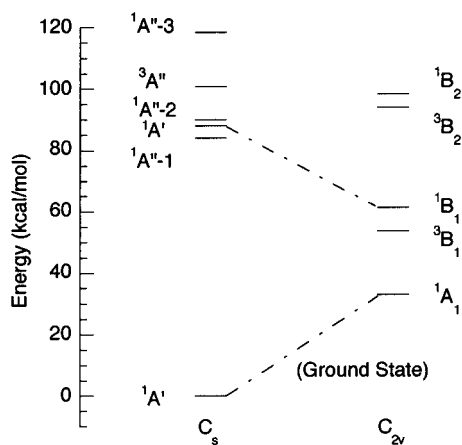**TABLE 2: Energies[a] of Optimized Geometries for H₂SO, MCQDPT/6-311+G(3df,2p)**

state	energy (Hartrees)	relative energy (kcal/mol)
ground state	−473.96104	0
ground state C_{2v} transition state	−473.90864	32.9
¹A′	−473.82059	88.1
¹A″−1	−473.82699	84.1
¹A″−2	−473.81754	90.0
¹A″−3	−473.77234	118.4
¹B₁	−473.86325	61.4
¹B₂	−473.80489	98.0
3A″	−473.80053	100.7
³B₁	−473.87526	53.8
³B₂	−473.81111	94.1

[a] ZPE not included.

believable, but not so for the optimized ¹A″ and ¹B₂ states. Instead, the orbitals for **¹A″-2** appeared to correlate better to the ¹B₂ state. (These data are shown in the Supporting Information.) Thus, only the ¹A′ to ¹B₁ excited state correlation line is shown in Figure 2. As shown below, the A″ path has many low lying states that result in forbidden crossings when the geometries are smoothly changed.

Least Linear Motion Pathways (LLMP) for H₂SO. It was hoped that once the vertical excited state for the ground state C_s geometry was correlated to the lower energy C_{2v} excited state, the states could be connected via an intrinsic reaction coordinate (IRC) method. The goal was to determine if the excited H₂SO (or DMSO, below) molecule could access the low energy C_{2v} geometries with low or minimal barriers. No transition states were located. As with the excited state Hessians (and for similar reasons), all attempts to get IRCs failed. Therefore, the best compromise to connect the geometries was to use least linear motion pathways. The LLMPs should provide upper bounds on the barriers, since they take sensible, but not necessarily ideal, paths from one stationary point to another.

Though several LLMPs could be constructed, the most physically reasonable is that which connects the vertical excited states to the relaxed planar geometries. This allows one to determine if there is a substantial barrier between the geometry at which the molecule is promoted to a given excited state by absorption and the low-energy planar minimum.

A 10-step LLMP was constructed from the vertical geometry to each of the relaxed planar geometries (i.e., ¹B₁, ¹B₂, ³B₁, and ³B₂). Careful CASSCF calculations, followed by MCQDPT correction of the energies gave energies of the A′ and A″ states at each point intermediate between the vertical and relaxed geometries, as illustrated in Figure 3. The excited ¹A′ state is, of course, the second state of that symmetry, and convergence of the MCSCF on such states is, in general, more difficult than convergence on the lowest state of a given symmetry. We were not able to achieve convergence at points 8 and 9 on the ¹A′ path. Nonetheless, the salient result here is that all four states show a path from the vertical excitation geometry to their respective planar geometries, along which there is no significant barrier.

Close analysis of the approximately singly occupied natural orbitals along the A′ to B₁ pathways of both multiplicities showed a smooth conversion of geometries and orbitals, indicating that the states are genuinely correlated. Both the singlet and triplet A″ pathways are not so well behaved. On the singlet surface, there is an inflection in the smooth curve between points 2 and 3. This coincides with a sudden change in appearance of the singly occupied orbitals between those two
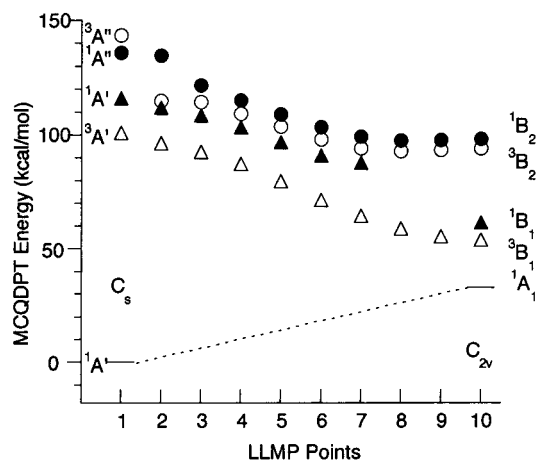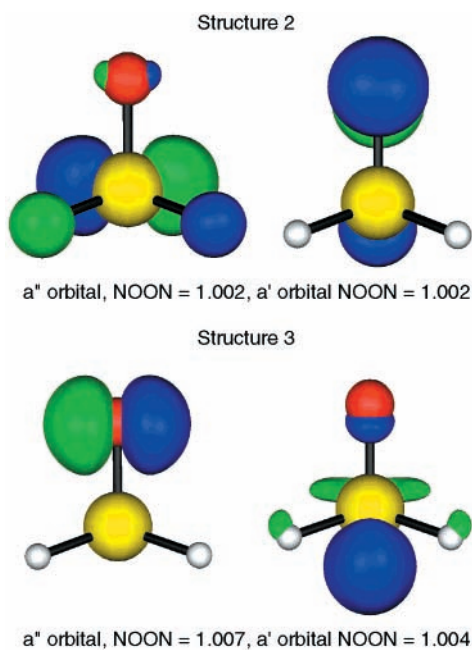

Figure 2. MCQDPT/6-311+G(3df,2p) energies of optimized geometries in C_s and C_{2v} symmetry, relative to the energy of the equilibrium ground state structure.

C_{2v} symmetry are similar to their singlet counterparts and are shown in the Supporting Information. The MCQDPT energies of all the geometry-optimized states are illustrated in Figure 2 and listed in Table 2.

In Figure 1, potential correlations between states of the same symmetry are drawn. These can be tested by inspection of the singly occupied orbitals. Examination of the orbitals for the "vertical" ¹A′ and ¹B₁ states made such a correlation quite

Figure 3. LLMP for H_2SO singlet vertical to relaxed geometry pathways. Circles are the A″ states and triangles are the A′ states. Hollow markers represent triplet states and filled markers are singlet states.

SCHEME 4: Singly Occupied Natural Orbitals along the $^1A''$ LLMP, Points 2 and 3[a]

Structure 2

a″ orbital, NOON = 1.002, a' orbital NOON = 1.002

Structure 3

a″ orbital, NOON = 1.007, a' orbital NOON = 1.004

[a] The orbital phases are indicated by colors blue and green. The change in state is illustrated by discontinuous change in orbitals.

points, as illustrated in Scheme 4, and is interpreted as a forbidden crossing with another low-lying $^1A''$ state.

This led to the calculation of an eight-point state-averaged LLMP pathway in $^1A'$ and $^1A''$ symmetry, in which the two lowest excited states of each symmetry were weighted equally. The results are shown in Figure 4. The $^1A'$ states are all far apart from each other and are well behaved. However, on the $^1A''$ surface the first two points are very close in energy (<10 kcal/mol) apart. These are the two states involved in the avoided crossing between points 2 and 3 in Figure 4. In addition, in Figure 4 at point 6 on the highest energy A″ surface, there looks to be another even higher lying A″ state close in energy, though this was not confirmed by averaging in the third highest A″ state.

DMSO. The behavior of the DMSO system was qualitatively quite similar to that of H_2SO. The $^1A'$ and $^3A'$ states of DMSO were found to correlate with the corresponding vertical B_1 states
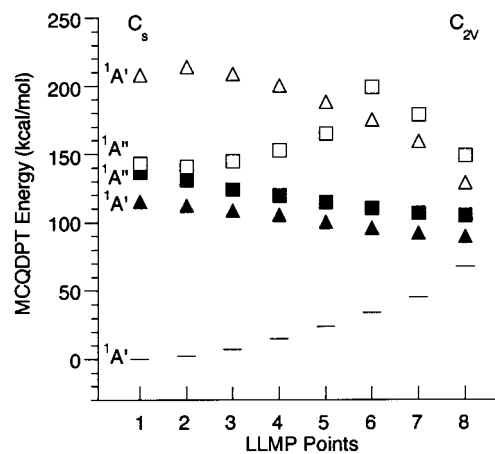

Figure 4. State averaged LLMP for H_2SO.

of the C_{2v} geometry. In addition, the $^1A''$ and $^3A''$ states were found to correlate with the vertical B_2 states of C_{2v} geometry. At the equilibrium geometry of DMSO, the vertical excitation energies should correspond to the λ_{max} of absorption bands. At MCQDPT/6-311+G(3df,2p), the lowest lying vertical singlet state ($^1A''$) is 132 kcal/mol above the ground state ($\lambda_{max} = 217$ nm). The $^1A'$ state was found lie 137 kcal/mol above the ground state, corresponding to $\lambda_{max} = 209$ nm. These values are in good agreement with the experimental absorption spectrum that has been deconvoluted, producing two bands with λ_{max} at 204 and 218 nm.[48] The lowest vertical triplet is $^3A'$, at 109 kcal/mol above the ground state, while the $^3A''$ state is just a few kcal/mol higher.

Relaxed excited state geometries were obtained by finding stationary points on the excited state surfaces. Again, Hessians were attempted without success. Only a single $^1A''$ state was found on this system, though we certainly do not rule out other bound structures existing. As shown in Scheme 5, the observed $^1A''$ state geometry is quite analogous to the lowest relaxed $^1A''$ state geometry of H_2SO, with an extended S−O bond and approximately normal C−S bond lengths. The $^1A'$ geometry is remarkably similar. The stationary points of $^1B_1$ and $^1B_2$ symmetry are also quite analogous to the H_2SO structures.

Two bound triplet structures were located. Both had C_{2v} symmetry and are analogous to the respective H_2SO structures. They are also shown in Scheme 5. Attempts to find a relaxed triplet geometry in C_s symmetry (i.e., based on or near the ground state geometry) universally resulted in dissociation to dimethyl sulfide and $O(^3P)$.[49] The energies of the relaxed excited states calculated for DMSO are shown in Figure 5. Only one correlation line is drawn that connects excited states, i.e., $^1A'$ to $^1B_1$. This is for the same reason as with H_2SO; the $^1A''$ surface is complex due to other low lying states with the same symmetry. It is also worth noting that, after geometrical relaxation, the $^1A''$ state has slipped below the $^1A'$, which is the lowest energy state at the ground state geometry.

Vertical Geometry to Relaxed Geometry for DMSO. A LLMP was constructed along the $^1A'$ and $^1A''$ surfaces from the ground state geometry to the relaxed $^1B_1$ and $^1B_2$ geometries, respectively. The results are shown in Figure 6. The triplet LLMP looks qualitatively very similar and can be found in the Supporting Information. Convergence of the CASSCF wave function was again a problem for some points closer to the relaxed triplet geometry on the $^1A'$ potential.

As with H_2SO, both the singlet and triplet A″ states are not well behaved, in that there are forbidden crossings. Switches

Ground and Excited State Potentials of DMSO and H₂SO

J. Phys. Chem. A, Vol. 105, No. 46, 2001 **10593**

SCHEME 5: Excited State Relaxed Geometries for DMSO Calculated at CASSCF[14,10]/6-311+G(3df)[a]

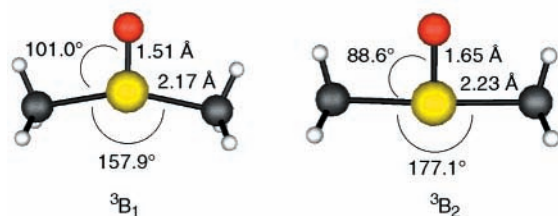Singlet geometries for DMSO
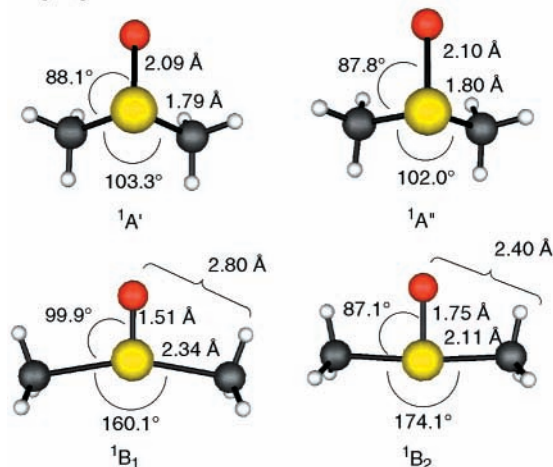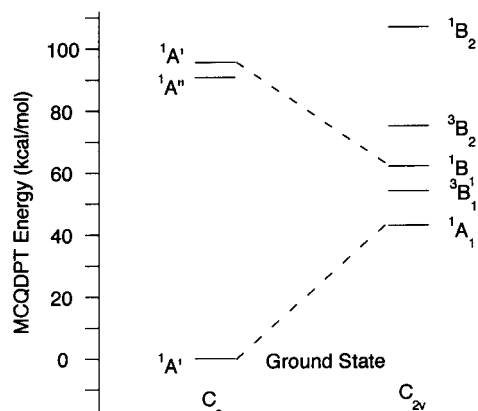

Triplet geometries for DMSO

[a] Braces indicate H−O bond distances.

Figure 5. Energetics of relaxed excited state geometries for DMSO at MCQDPT/6-311+G(3df,2p). The ground state equilibrium geometry is set to zero energy.

in the singly occupied orbitals similar to those illustrated in Scheme 4 are observed between the third and fourth points along the A″ path on both the singlet and triplet surface. Despite its not-quite-monotonic behavior, the A′ path is well behaved.

Finally, it should be pointed out that the abscissa of Figure 6 and those like it is somewhat misleading in that the geometries of the molecules are not identical. In particular, the geometries of the C_{2v} structures are not the same. It is thus important to know the energy of the ground electronic state at the geometry of the $^1B_1$ stationary point in order to know how close the surfaces are at that place in conformation space. Neglecting zero point energies (because they could not be obtained for the excited states), the calculated gap between the ground $^1A_1$ and $^1B_1$ surfaces at the optimized $^1B_1$ geometry is 6.0 kcal/mol, as seen in Table 3.
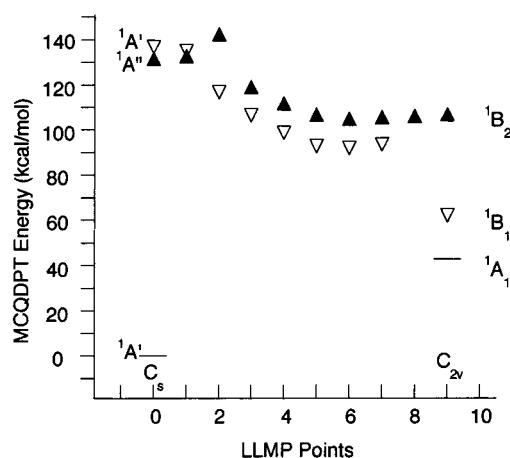

Figure 6. LLMP for DMSO singlet vertical geometry to relaxed geometry pathways.

TABLE 3: DMSO Energies, MCQDPT/6-311+G(3df)

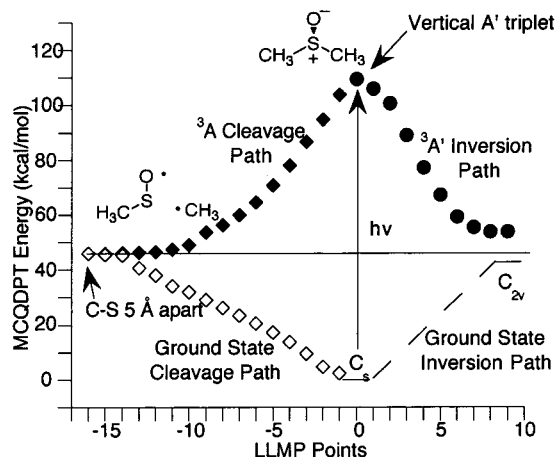| state	energy (Hartrees)	relative energy (kcal/mol)[a]
relaxed ground state ($^1A_1$)	−552.39172	0
ground C_{2v} transition state ($^1A_1$)	−552.32333	42.9[a]
relaxed $^1B_1$ state	−552.29295	62.0
ground state ($^1A_1$) at $^1B_1$ geometry	−552.30247	56.0

[a] ZPE not included.

Figure 7. Triplet inversion and α-cleavage pathways for DMSO beginning from the vertical $^3A'$ state.

Inversion Pathway versus α-Cleavage Pathway for DMSO. The bond dissociation energy for the carbon−sulfur bond is about 53 kcal/mol; thus any of the excited states discussed here easily contains enough energy to cleave one of the C−S bonds. Indeed, the experimental observation on gas-phase photolysis of DMSO is the production of CH₃SO• and CH₃•.[24,48]

A comparison of the inversion and α-cleavage triplet pathways is shown in Figure 7. For consistency, we attempted to get the same information for the singlet pathway. However, as soon as one C−S bond is stretched, all symmetry is lost, and convergence on excited states is difficult. On the other hand, the "ground triplet" state is precisely what is wanted on that spin manifold. Three paths were calculated in a point by point manner. An optimized geometry with a constrained C−S "bond" distance of 5.0 Å was obtained. A LLMP was constructed from there to the ground state geometry. No significant barrier is observed among points calculated for the lowest triplet state along that path. For a ground state α-cleavage surface, constrained optimizations at fixed C−S bond distances were

10594 *J. Phys. Chem. A, Vol. 105, No. 46, 2001*

Cubbage and Jenks

carried out. At this level of theory (still neglecting ZPE), the BDE of the C—S bond is 46.2 kcal/mol, which is essentially invariant to stretching the distance to 20 Å. Previous calculations at the G2(MP2) level get a more accurate number of 53 kcal/mol.[24]

Discussion

Ground State Inversion. The inversion barriers and geometries calculated at the MP2/6-311+G(3df,2p) level of theory compare well with those of Fueno et al.[18] Small differences between those values and the present ones derive from the somewhat smaller basis sets used by the previous workers. Regardless, it was found that more realistic[50] energies are calculated with multireference techniques. However, the lack of experimental activation data for simple dialkyl sulfoxide racemization is unfortunate. Given that there are often quantitative differences between characteristics of alkyl and aryl sulfoxides, it is not clear how to assess the quantitative accuracy of the current calculated number.

Excited States and Inversion. As seen above, H_2SO and DMSO produced similar excited state pictures. The most essential result of this work is that both species have low energy excited state structures with C_{2v} symmetry, lending further credibility to the hypothesis that excitation of sulfoxides can lead to stereomutation without going through radical intermediates. As shown in Table 3, the energies of the ground and first excited singlet states are within about 6 kcal/mol of one another at the geometry of the T-shaped relaxed singlet excited state; the gap is larger at the geometry of the ground transition state. While we have no specific evidence of a conical intersection connecting the two states, it seems safe to speculate that $^1B_1$ state with its planar geometry can act as a funnel from which efficient transition to the ground state and subsequent randomization of the sulfur stereochemistry (in asymmetric derivatives of DMSO) can occur.

We have not constructed full energy surfaces and conducted molecular dynamics simulations, so the calculations here do not serve as a basis to describe the partitioning among possible processes available to excited state H_2SO and DMSO. Given the symmetry breaking inherent in numerical calculation of vibrational data, we were not even able to prove that the excited state stationary points are all minima. However, it seems clear that the C_{2v} structures are minima, given that C_s structures at geometries only slightly distorted from that stationary point had higher energies. Thus, the current data are consistent with the mechanism originally suggested in Scheme 1, with a few caveats. First, there are excited state minima (or at least stationary points) other than the low energy one with high symmetry. Second, there may be no bound structures on the triplet surface, at least in the vicinity of the ground state conformation, and finally, a pathway that leads to α-cleavage must be included.

This general scheme is consistent with the generally observed low fluorescence yields for a number of arenes with sulfinyl substitution,[30−32] though such aromatic cases are clearly more complex than these. Further study is required before such an extension can be seen as more than speculative.

Conclusions

This study presents the first computational prediction of excited state geometries of sulfoxides. For H_2SO and DMSO, there are excited state stationary points with C_{2v} symmetry. The LLMP calculations suggest that there is little if any energy barrier along the path from the vertical geometry in excited states of either $^1A'$ or $^1A''$ symmetry. The lowest energy of these

relaxed excited state geometries for DMSO is a mere 6 kcal/mol above the ground state at that same geometry, which strongly suggests that nonradiative decay to the ground state would be extremely efficient in that vicinity of conformation space. This provides the electronic basis for a sulfur inversion mechanism that does not involve the formation of radicals.

Supporting Information Available: Triplet relaxed geometries for H_2SO, orbital illustrations, additional LLMP calculations, coordinates and absolute calculated energies. Supporting Information is available free of charge via the Internet at www.pubs.acs.org.

References and Notes

(1) Dobado, J. A.; Martinez-Garcia, H.; Molina, J. M.; Sundberg, M. R. *J. Am. Chem. Soc.* **1999**, *121*, 3156−3164.

(2) Andersen, K. K. Stereochemistry, Conformation, and Chiroptical Properties of Sulfoxides. In *The Chemistry of Sufoxides and Sulfones*; Patai, S., Rappoport, Z., Stirling, C. J. M., Eds.; John Wiley & Sons Ltd.: New York, 1988; pp 55−94.

(3) Allin, S. M. *Organosulfur Chem.* **1998**, *2*, 41−61.

(4) Skarzewski, J.; Ostrycharz, E. *Wiad. Chem.* **2000**, *54*, 725−758.

(5) Rayner, D. R.; Gordon, A. J.; Mislow, K. *J. Am. Chem. Soc.* **1968**, *90*, 4854−4860.

(6) Carreño, M. C. *Chem. Rev.* **1995**, *95*, 1717−1760.

(7) Carretero, J. C.; Arrayas, R. G.; Buezo, N. D.; Garrido, J. L.; Alonso, I.; Adrio, J. *Phosphorus, Sulfur Silicon Relat. Elem.* **1999**, *153−154*, 259−273.

(8) Metzner, P.; Alayrac, C.; Julienne, K.; Nowaczyk, S. *Actual. Chim.* **2000**, 54−59.

(9) Bravo, P.; Zanda, M. *Enantiocontrolled Synth. Fluoro-Org. Compd.* **1999**, 107−160.

(10) Matsuyama, H. *Sulfur Rep.* **1999**, *22*, 85−121.

(11) Allin, S. M.; Shuttleworth, S. J.; Bulman Page, P. C. *Organosulfur Chem.* **1998**, *2*, 97−155.

(12) Krafft, F.; Lyons, R. E. *Chem. Ber.* **1896**, *29*, 435−436.

(13) Mislow, K. *Rec. Chem. Prog.* **1967**, *28*, 216−40.

(14) Kingsbury, C. A.; Cram, D. J. *J. Am. Chem. Soc.* **1960**, *82*, 1810−1819.

(15) Emerson, W. W.; Craig, A. P.; Potts, I. W., Jr. *J. Org. Chem.* **1967**, *32*.

(16) Yoshimura, T.; Tsukurimichi, E.; Iizuka, Y.; Mizuno, H.; Isaji, H.; Shimasaki, C. *Bull. Chem. Soc. Jpn.* **1989**, *62*, 1891−1899.

(17) Cubbage, J. W.; Guo, Y.; McCulla, R. D.; Jenks, W. S. Submitted for publication.

(18) Fueno, H.; Ikuta, S.; Masuyama, H.; Kamigata, N. *J. Chem. Soc., Perkin Trans. 2* **1992**, 1925−1928.

(19) Arduengo, A. J., III; Stewart, C. A. *Chem. Rev. (Washington, D.C.)* **1994**, *94*, 1215−37.

(20) Bickart, P.; Carson, F. W.; Jacobus, J.; Miller, E. G.; Mislow, K. *J. Am. Chem. Soc.* **1968**, *90*, 4869−4876.

(21) Miller, E. G.; Rayner, D. R.; Thomas, H. T.; Mislow, K. *J. Am. Chem. Soc.* **1968**, *90*, 4861−4868.

(22) Mislow, K.; Axelrod, M.; Rayner, D. R.; Gottardt, H.; Coyne, L. M.; Hammond, G. S. *J. Am. Chem. Soc.* **1965**, *87*, 4958−4959.

(23) Still, I. W. J. Photochemistry of Sulfoxides and Sulfones. In *The Chemistry of Sulfones and Sulfoxides*; Patai, S., Rappaport, Z., Stirling, C. J. M., Eds.; John Wiley & Sons Ltd.: New York, 1988; pp 873−887.

(24) Zhao, H.-Q.; Cheung, Y.-S.; Heck, D. P.; Ng, C. Y.; Tetzlaff, T.; Jenks, W. S. *J. Chem. Phys.* **1997**, *106*, 86−93.

(25) Darmanyan, A. P.; Gregory, D. D.; Guo, Y.; Jenks, W. S. *J. Phys. Chem. A* **1997**, *101*, 6855−6863.

(26) Guo, Y.; Jenks, W. S. *J. Org. Chem.* **1997**, *62*, 857−864.

(27) Jenks, W. S.; Gregory, D. D.; Guo, Y.; Lee, W.; Tetzlaff, T. Photochemistry of Sulfoxides and Related Compounds. In *Organic Photochemistry*; Ramamurthy, V., Schanze, K. S., Eds.; Marcel Dekker: New York, 1997; Vol. 1, pp 1−56.

(28) Kropp, P. J.; Fryxell, G. E.; Tubergen, M. W.; Hager, M. W.; Harris, G. D., Jr.; McDermott, T. P., Jr.; Tornero-Velez, R. *J. Am. Chem. Soc.* **1991**, *113*, 7300−7310.

(29) Schultz, A. G.; Schlessinger, R. H. *J. Chem. Soc. Chem. Commun.* **1970**, 1294−1295.

(30) Tsurutani, Y.; Yamashita, T.; Horie, K. *Polym. J.* **1998**, *30*, 11−16.

(31) Tsurutani, Y.; Machida, S.; Horie, K.; Kawashima, Y.; Nakano, H.; Hirao, K. *J. Photochem. Photobiol., A* **1999**, *122*, 161−168.

(32) Lee, W.; Jenks, W. S. *J. Org. Chem.* **2001**, *66*, 474−480.

(33) Ganter, C.; Moser, J.-F. *Helv. Chim. Acta* **1971**, *54*, 2228−2251.

(34) Spry, D. O. *J. Am. Chem. Soc.* **1970**, *92*, 5006−5008.

(35) Archer, R. A.; Kitchell, B. S. *J. Am. Chem. Soc.* **1966**, *88*, 3462−3463.

(36) Kishi, M.; Komeno, T. *Tetrahedron Lett.* **1971**, *28*, 2641−2644.

(37) Schmidt, M. W.; Baldridge, K. K.; Boatz, J. A.; Elbert, S. T.; Gordon, M. S.; Jensen, J. H.; Koseki, S.; Matsunaga, N.; Nguyen, N.; Su, S. J.; Windus, T. L.; Dupuis, M.; Montgomery, J. A. *J. Comput. Chem.* **1993**, *14*, 1347−1363.

(38) Bode, B. M.; Gordon, M. S. *J. Mol. Graphics. Mod.* **1998**, *16*, 133−138.

(39) Boys, S. F. *Quantum Theory At., Mol., Solid State* **1966**, 253−62.

(40) Schmidt, M.; Gordon, M. S. *Annu. Rev. Phys. Chem.* **1998**, *49*, 233−266.

(41) Schmidt, M. W.; Gordon, M. S. *Ann. Rev. Phys. Chem.* **1998**, *49*, 233−266.

(42) Roos, B. O. The Multiconfiguration SCF Methodol. In *Methods in Computational Molecular Physics*; Kiercksen, G. H. F., Wilson, S., Eds.; D. Reidel: Dordrecht, The Netherlands, 1983.

(43) Nakano, H. *Chem. Phys. Lett.* **1993**, *207*, 372−378.

(44) Nakano, H. *J. Chem. Phys.* **1993**, *99*, 7983−7992.

(45) Chaban, G.; Schmidt, M. W.; Gordon, M. S. *Theor. Chem. Acc.* **1997**, *97*, 88−95.

(46) Lengsfield, B. H., III. *J. Chem. Phys.* **1980**, *73*, 382−390.

(47) Hargittai, I. Structural Chemistry of Gaseous Sulfoxides and Sulfones. In *The Chemistry of Sulfones and Sulfoxides*; Patai, S., Rappoport, Z., Stirling, C. J. M., Eds.; John Wiley & Sons Ltd.: New York, 1988; pp 33−53.

(48) Thorson, G. M.; Cheatum, C. M.; Coffey, M. J.; Crim, F. F. *J. Chem. Phys.* **1999**, *110*, 10843−10849.

(49) We cannot rule out the existence of such stationary points. We can only state that we were unable to find any.

(50) Toyota, S. *Rev. Heteroatom Chem.* **1999**, *21*, 139−162.